Proteasomal degradation of Sfp1 contributes to the repression of ribosome biogenesis during starvation and is mediated by the proteasome activator Blm10

Antonio Diaz Lopez*,†, Krisztina Tar*, Undine Krügel, Thomas Dange‡, Ignacio Guerrero Ros, and Marion Schmidt*
Department of Biochemistry, Albert Einstein College of Medicine, Bronx, NY 10461

ABSTRACT **The regulation of ribosomal protein (RP) gene transcription is tightly linked to the nutrient status of the cell and is under the control of metabolic signaling pathways. In *Saccharomyces cerevisiae* several transcriptional activators mediate efficient RP gene transcription during logarithmic growth and dissociate from RP gene promoters upon nutrient limitation. Repression of RP gene transcription appears to be regulated predominantly by posttranslational modification and cellular localization of transcriptional activators. We report here that one of these factors, Sfp1, is degraded by the proteasome and that the proteasome activator Blm10 is required for regulated Sfp1 degradation. Loss of Blm10 results in the stabilization and increased nuclear abundance of Sfp1 during nutrient limitation, increased transcription of RP genes, increased levels of RPs, and decreased rapamycin-induced repression of RP genes. Thus we conclude that proteasomal degradation of Sfp1 is mediated by Blm10 and contributes to the repression of ribosome biogenesis under nutrient depletion.**

Monitoring Editor
Thomas Sommer
Max Delbrück Center for Molecular Medicine

Received: Apr 26, 2010
Revised: Dec 6, 2010
Accepted: Dec 20, 2010

INTRODUCTION

The proteasome is an essential protease in the cytoplasm and nuclei of eukaryotic cells. It consists of two entities: a central proteolytic core (the 20S proteasome in higher eukaryotes or the core particle [CP] in *Saccharomyces cerevisiae*) and a regulatory or activating complex. The CP has a barrel-shaped topology formed by four stacked rings (two inner β and two outer α rings), composed of seven subunits each. The β rings harbor three different proteolytically active subunits with different specificities: trypsin-like, chymotrypsin-like, and postacidic activity (Kisselev *et al.*, 2006). The active sites are sequestered within the interior of the CP barrel (Groll *et al.*, 1997). Access to the proteolytic chamber is controlled by an adjustable gate and is mediated by proteasome regulators/activators (Foerster *et al.*, 2003). Three activator families have been described: the conserved regulatory particle (19S or PA700), the PA28 family (REG, 11S regulator) (Li and Rechsteiner, 2001), and the conserved Blm10/PA200 proteins (Ustrell *et al.*, 2002; Schmidt *et al.*, 2005), providing a variety of different proteasomal subspecies, which most likely target different groups of proteasomal substrates. The regulatory particle consists of 19 subunits, among them six paralogous ATPases (Finley, 2009). Opening of the CP gate by the RP is achieved by insertion of the ATPase C-termini into specific pockets at the CP surface (Smith *et al.*, 2007; Gillette *et al.*, 2008; Stadtmueller *et al.*, 2009). PA28 activators are characterized by a hepta- or hexa-oligomeric ring structure of ~200 kDa (Rechsteiner and Hill, 2005). The C-termini of the subunits of PA28 are inserted into the same α subunit pockets as the C-termini of the ATPases. However, C-terminal docking of the PA28 subunits does not trigger gate opening. Instead, internal segments known as the PA28 activation loops induce a structural rearrangement of the gate region, which allows substrate entry (Whitby *et al.*, 2000).

This article was published online ahead of print in MBoC in Press (http://www.molbiolcell.org/cgi/doi/10.1091/mbc.E10-04-0352) on January 5, 2011.

*These authors contributed equally to this work.

Present addresses: †Instituto de Investigaciones Biomedicas, GSIC-UAM, Universidad Autonoma de Madrid, 28029 Madrid, Spain; ‡Department of BioNanoScience, Kavli Institute of NanoScience, Technical University Delft, Lorentzweg, 2628 CJ Delft, The Netherlands.

Address correspondence to: Marion Schmidt (marion.schmidt@einstein.yu.edu).

Abbreviations used: CHX. cycloheximide; CP, core particle; C_T, cycle threshold; DIC, differential interference contrast; DMSO, dimethyl sulfoxide; GFP, green fluorescent protein; HA; hemagglutinin; log; logarithmic; PDS, postdiauxic shift; Pgk1, phosphoglycerate kinase 1; PKA, cyclic AMP–dependent kinase A; qRT-PCR, quantitative real-time PCR; RP, ribosomal protein; stat, stationary; Suc-LLVY-AMC, *N*-succinyl-Leu-Leu-Val-Tyr-7-amino-4-methylcoumarin; TEV, tobacco etch virus; TOR, target of rapamycin; WT, wild type; YPD, yeast peptone dextrose.

Blm10 in *S. cerevisiae* and its human orthologue PA200 are large ~245-kDa proteins composed of HEAT repeats, which associate with the CP/20S gate region (Ortega *et al.*, 2005; Schmidt *et al.*, 2005; Iwanczyk *et al.*, 2006; Sadre-Bazzaz *et al.*, 2010). In mammalian cells PA200 was found exclusively in a complex with the proteasome (Blickwedehl *et al.*, 2008). We have demonstrated recently that in rapidly growing yeast cells Blm10 is part of a mature proteasome hybrid complex, where Blm10 occupies one end of the core cylinder and the regulatory particle the other end (Schmidt *et al.*, 2005). Blm10–CP devoid of regulatory particles was not detected in unfractionated lysates, suggesting that the dominant species of Blm10-containing proteasomes is the hybrid complex. Blm10–CP complexes, purified after the dissociation of the regulatory particle from the hybrid complex, exhibit elevated CP peptidase activity (Schmidt *et al.*, 2005; Iwanczyk *et al.*, 2006; Li *et al.*, 2007; Lehmann *et al.*, 2008). Both hybrid complex formation and activation of the proteasome peptidase activity have also been described for PA200–proteasome complexes (Ustrell *et al.*, 2002; Blickwedehl *et al.*, 2008), suggesting that Blm10/PA200 proteins might represent a novel conserved monomeric proteasome activator family. A recent structural analysis of $Blm10_2$-CP complexes showed that similar to RP and PA28, Blm10 binding to the CP is mediated via its C-terminus. The C-terminal Blm10 residues cause structural alterations within the gate region, resulting in a partially open, disordered gate in a molecular mechanism that appears to be similar to the C-terminal docking of the proteasomal ATPases, but different from PA26 C-terminal binding to the CP, which per se does not induce gate opening (Sadre-Bazzaz *et al.*, 2010). Furthermore, a pore within Blm10 of 13–22 Å has been detected. Whether these structural characteristics of Blm10–CP complexes are sufficient to promote protein degradation remains to be established.

The cellular functions of Blm10 are poorly understood. A proposed role for Blm10/PA200 in DNA repair (Febres *et al.*, 2001; Ustrell *et al.*, 2002) was not confirmed in subsequent studies in yeast and in mammalian cells (Schmidt *et al.*, 2005; Khor *et al.*, 2006; McCullock *et al.*, 2006). In *S. cerevisiae* Blm10 binding to the proteasome occurs at a late stage during proteasome maturation (Fehlker *et al.*, 2003; Li *et al.*, 2007; Marques *et al.*, 2007), which initially suggested a possible function in proteasome assembly. Loss of *BLM10*, however, does not result in a significant defect in proteasome assembly (Marques *et al.*, 2007) or in gross changes in mature proteasome populations (Schmidt *et al.*, 2005). Double mutants that combine loss of *BLM10* and an assembly-defective proteasomal regulatory particle mutant show defects in 20S maturation, while either single mutant does not (Marques *et al.*, 2007). Thus activator binding to immature CP complexes (either the regulatory particle or Blm10) appears to be an integral part of CP maturation, with Blm10 and the regulatory particle playing redundant roles during this process.

The regulation of ribosome abundance and output is crucial for the maintenance of the energy economy within a cell and thus for cell growth and size. It is estimated that ribosome biosynthesis accounts for ~70% of total transcription and ~25% of the total translation in rapidly growing yeast cells (Warner, 1999; Rudra *et al.*, 2005). Thus ribosome function and biogenesis have to be tightly correlated with the cellular nutrient status. This process is mediated by the activity of the major metabolic signaling pathways, the target of rapamycin kinase (TORC1), and cyclic AMP–dependent kinase A (PKA) pathways. Inactivation of TORC1 or PKA in yeast in response to limiting nutrients results in rapid repression of ribosomal genes and inhibition of translation (Powers and Walter, 1999; Wullschleger *et al.*, 2005). Ribosome biogenesis requires the activity of all three nuclear RNA polymerases, which mediate the expression of ribosomal proteins (RPs), rRNAs, and accessory proteins, which assist in ribosome assembly. In *S. cerevisiae* factors controlling ribosomal gene expression include Rrn3, regulating Pol I–driven genes (Claypool *et al.*, 2004); Maf1, which acts upon Pol III–mediated transcription (Upadhya *et al.*, 2002); and the Pol II–directed transcriptional regulators Rap1, Ifh1, Fhl1, Hmo1, and Sfp1 (Fingerman *et al.*, 2003; Jorgensen *et al.*, 2004; Marion *et al.*, 2004; Martin *et al.*, 2004; Schawalder *et al.*, 2004; Wade *et al.*, 2004; Zhao *et al.*, 2006; Berger *et al.*, 2007). Although TORC1/PKA signaling pathways have been implicated in the regulation of some of these factors, the precise mechanisms of gene activation and repression are not completely understood.

In this report we provide evidence for a regulatory function of proteasome-mediated turnover of Sfp1 in the repression of ribosome biogenesis upon nutrient depletion. Additionally, we demonstrate that proteasome-dependent Sfp1 turnover is mediated by the proteasome activator Blm10.

RESULTS

BLM10 deletion results in resistance to sublethal doses of cycloheximide

To gain insight into the cellular functions of Blm10, we performed a screen for loss-of-function phenotypes of cells deleted for *BLM10*. We found that *blm10*Δ cells exhibit resistance to sublethal doses of the translational inhibitor cycloheximide (CHX) (Figure 1A). The same phenotype has been associated with proteasome CP and regulatory particle mutants (*crl* mutants) defective in the turnover of ubiquitin conjugates (Gerlinger *et al.*, 1997), derived from a screen for CHX-resistant yeast mutants (McCusker and Haber, 1988). Similar observations have been made in *Arabidopsis thaliana* (Kurepa *et al.*, 2010). To corroborate that CHX resistance is a general phenotype of proteasome loss-of-function mutants, we tested the growth of the proteasomal ATPase mutants *rpt1S*, *rpt2RF*, and *rpt3R* (Rubin *et al.*, 1998) under the same conditions. The respective point mutations prevent nucleotide binding to the ATPase subunits due to a point mutation within the Walker A motif, yet still allow cell growth. The ATPase mutants showed similar CHX resistance as loss of *BLM10* (Figure 1A, bottom).

Ubp6 is a negative regulator of proteasome function, and *ubp6*Δ cells are characterized by proteasome hyperactivity (Hanna *et al.*, 2003, 2006). In contrast to proteasome hypomorphs such as the ATPase mutants, loss of *UBP6* results in strong CHX sensitivity (Figure 1A, middle). Interestingly, loss of *UBP6* confers resistance to a second translation inhibitor, hygromycin B (Hanna *et al.*, 2003). The same opposing phenotype between CHX and hygromycin B is observed for loss of *BLM10* or for the ATPase mutants *rpt1S*, *rpt2SF*, and to a lesser extent *rpt3R* (Figure 1A, right), yet sensitivity and resistance to the drugs are inverted as compared with *ubp6*Δ. We conclude that proteasome loss-of-function mutants (ATPase mutants) confer CHX resistance and sensitivity to hygromycin B, while proteasome hyperactivity (*ubp6*Δ) results in the opposite phenotypes. It appears surprising that proteasome mutants are sensitive to one class of translation inhibitors but resistant to another. However, both inhibitors are chemically and mechanistically different. Hygromycin B is an aminoglycoside, which causes miscoding (Sutcliffe, 2005) and accumulation of misfolded proteins, explaining the sensitivity of mutants with reduced proteasomal activity. CHX, on the other hand, is a glutarimide antibiotic, which prevents initiation of translation, elongation, and the removal of the nascent chain from the ribosome. It furthermore inhibits polysome breakdown and reassembly (Pestka, 1971). Thus CHX-treated cells are characterized

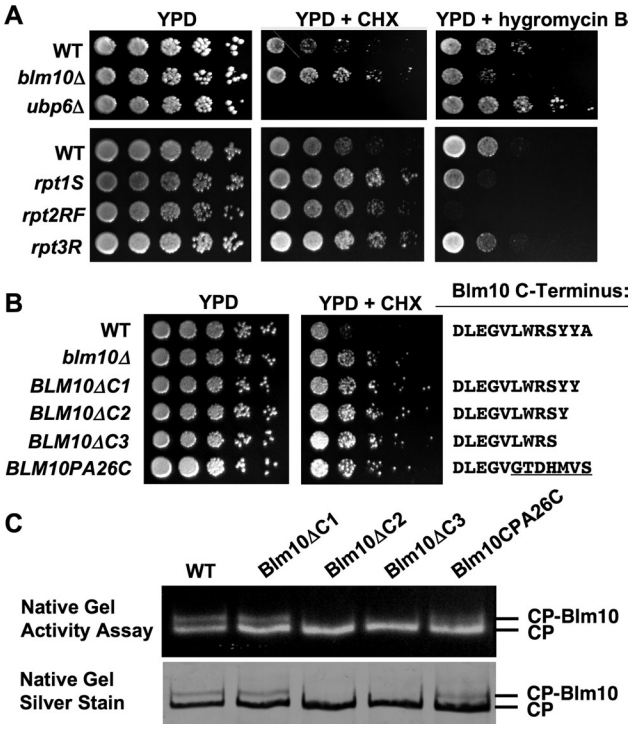

FIGURE 1: Loss of *BLM10* or disruption of its ability to bind to the proteasome results in cycloheximide (CHX) resistance. (A) Overnight cultures of WT (BY4741), *blm10*Δ (yMS63), and *ubp6*Δ (yMS222) cells (top) or WT (SUB62), *rpt1S* (DY106), *rpt2RF* (DY62), and *rpt3R* (DY93) (bottom) were serially diluted and spotted onto YPD in the absence or presence of 0.3 μg/ml (top) or 0.5 μg/ml (bottom) CHX or 60 μg/ml hygromycin B and incubated at 30°C for 2 d (YPD) or 4 d (CHX, hygromycin B). (B) C-terminal *Blm10* mutants exhibit a loss-of-function phenotype. Fivefold serial dilutions of overnight cultures of wild-type (WT) yeast strains, strains deleted for *BLM10* (*Δblm10*), strains with genomically integrated C-terminal deletion mutants (*BLM10ΔC1*, *BLM10ΔC2*, and *BLM10ΔC3*), and a chimeric Blm10 protein where the last seven residues were exchanged against the corresponding residues of PA26 (*BLM10PA26C*) were spotted on YPD in the absence (left) or in the presence of 0.3 μg CHX (right). The C-terminal sequences are indicated to the right. (C) Purified WT Blm10–CP and complexes with C-terminal Blm10 mutants as indicated in (B) were purified and subjected to native gel electrophoresis, followed by an in-gel activity assay with the fluorogenic proteasome substrate Suc-LLVY-AMC (top). Subsequently the gel was stained with silver nitrate (bottom). The positions of Blm10–CP and CP are indicated.

by reduced protein synthesis. Increased proteasome activity induced by loss of *UBP6* aggravates sensitivity to CHX, while proteasome loss of function alleviates the phenotype.

Because loss of *BLM10* results in the same phenotype as the proteasome hypomorphic ATPase mutants (CHX resistance and sensitivity to hygromycin B), we conclude that Blm10 positively regulates proteasome activity, providing evidence for its role as a proteasome activator.

BLM10 mutations, which prevent CP binding, exhibit a loss-of-function phenotype

Recently it was demonstrated that Blm10 interaction with the CP involves C-terminal docking of Blm10 to conserved binding pockets located at the upper surface of the CP barrel (Sadre-Bazzaz *et al.*, 2010). To investigate whether the CHX-resistant phenotype is related to the property of Blm10 to bind to the proteasome, we constructed a series of C-terminal *BLM10* deletions in which either the last residue (*BLM10ΔC1*), the last two residues (*BLM10ΔC2*), or the last three residues (*BLM10ΔC3*) were removed. All C-terminal mutants exhibited a CHX-resistant phenotype (Figure 1B), arguing for a model in which Blm10 function is linked to its association with the proteasome. To corroborate that the mutations affect Blm10 binding to the proteasome, we purified Blm10–CP complexes and resolved them on native gels. While the deletion of the last residue of Blm10 still allowed complex formation, deletion of the last two or three residues abolished Blm10 association with the CP (Figure 1C). Interestingly, although deletion of the last residue did not prevent proteasome binding (Figure 1C), it caused a loss-of-function phenotype (Figure 1B), which could indicate that the C-terminus of Blm10 might have additional roles beyond CP binding. The same observation, intact complex formation plus a loss-of-function phenotype, is evident for a C-terminal chimera, where the last seven residues of Blm10 were exchanged against the C-terminal residues of PA26 (Figure 1, B and C).

Loss of Blm10 affects the abundance of RPs after the diauxic shift

We hypothesized that the CHX-resistant phenotypes upon loss of *BLM10* or inactive ATPases might be a consequence of improved ribosome function, for example, due to increased ribosome levels. The control of ribosome abundance is a highly regulated process that is sensitive to the metabolic status of the cell. *S. cerevisiae* growth is characterized by three defined metabolic phases, as highlighted in Figure 2A (Gasch and Werner-Washburne, 2002; Herman, 2002). Initially, yeast cells grow logarithmically and generate ATP by fermentation (logarithmic [log] phase). On nutrient depletion, ATP is generated by oxidative metabolism. This switch from fermentation to oxidative metabolism is known as the "diauxic shift" and is marked by flattening of the growth curve (Figure 2A), indicative of a reduced growth rate. After several days in the postdiauxic shift (PDS) phase, cells arrest in G_0, also known as the stationary (stat) phase in yeast. Both ribosome biogenesis and abundance decrease strongly when cells pass the diauxic shift (PDS) or are treated with the Tor inhibitor rapamycin (Powers and Walter, 1999). To test for potential alterations in ribosome abundance in *blm10*Δ cells, we analyzed the steady-state levels of two RPs, Rpl3 (Figure 2B, top left) and Rpl30 (top right), in the different metabolic phases. As expected, RP levels are significantly reduced in PDS and stat phase (Figure 2B) in wild-type (WT) cells. A longer exposure of Figure 2B is shown in Supplemental Figure 1. Strikingly, after the diauxic shift and in stat phase, *BLM10*-deleted cells exhibit elevated steady-state levels of RPs (Figure 2B).

Because Blm10 activates the proteasome, a potential explanation for increased RP levels upon *BLM10* deletion after the diauxic shift is a participation of Blm10-proteasomes in RP turnover. To test this hypothesis, we performed CHX chase experiments in the presence of lethal doses of the drug (Kornitzer, 2002). Incubation with high doses of CHX blocks protein synthesis, allowing for determining the rate of protein turnover. Ribosomes are very stable complexes, with an estimated half-life of several days (Warner, 1999). *BLM10* deletion did not affect RP turnover (Figure 2C). Our findings are in agreement with a recent report that demonstrates that ribosome turnover is achieved via autophagy in a process involving the deubiquitinating enzyme Ubp3/Bre5 (Kraft *et al.*, 2008).

Loss of *BLM10* affects RP gene transcription

An alternative explanation for elevated RP levels in *BLM10*-deleted cells would be dysregulation of RP gene transcription. We therefore determined mRNA levels of five RP genes by quantitative real-time PCR (qRT-PCR) in WT and *blm10*Δ cells in the different growth

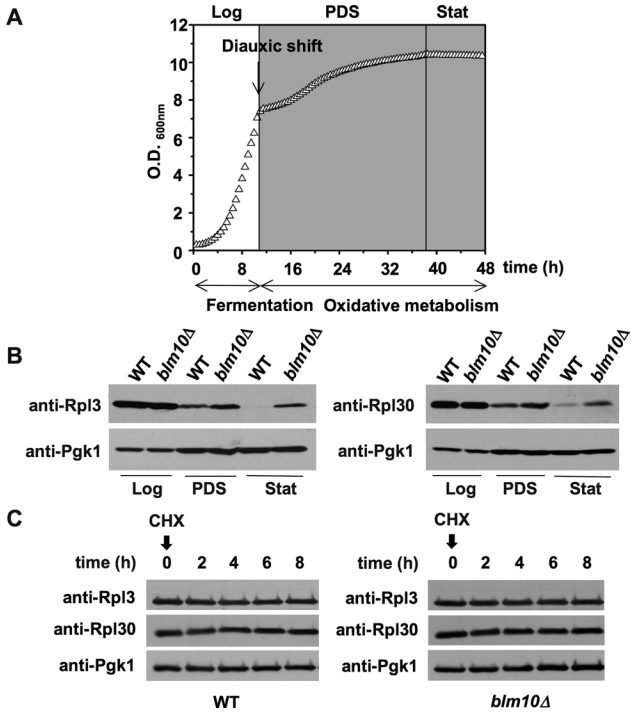

FIGURE 2: RP abundance is increased in *BLM10*-deleted cells. (A) Characteristic growth curve of WT (BY4741) yeast cells in YPD obtained in a Bioscreen C MB instrument. The relevant metabolic phases of yeast growth are indicated (log, logarithmic phase; PDS, postdiauxic shift phase; stat, stationary phase). (B) RP abundance is increased in PDS and stat in *BLM10*-deleted cells. WT (yMS268) and *blm10*Δ (yMS63) cells grown in YPD were harvested in the different metabolic phases (log, PDS, and stat) and lysed. Equal amounts of protein were subjected to SDS–PAGE, followed by immunodetection with Rpl3- (left) and Rpl30-specific (right) antisera. Immunodetection of phosphoglycerate kinase 1 (Pgk1) was used as loading control (bottom). (C) RP turnover is not affected by loss of *BLM10*. RP levels at the time points indicated were determined after inhibition of protein synthesis by addition of 200 µg/ml CHX to log phase WT (yMS683) or *blm10*Δ (yMS684) cells. Cell lysates were subjected to SDS–PAGE followed by immunodetection with Rpl3- or Rpl30-specific antibodies as indicated. Pgk1 protein levels were used as loading control (bottom).

phases. RP gene transcription is strongly repressed after the diauxic shift in WT cells (Figure 3A; Brauer *et al.*, 2005). Loss of *BLM10* did not affect RP gene transcription in log phase (Figure 3B), in agreement with unchanged RP levels observed under the same conditions (Figure 2B). After the diauxic shift, however, RP gene transcription was elevated in the absence of *BLM10* (Figure 3C).

RP gene transcription is rapidly down-regulated upon TORC1 inhibition by rapamycin (Powers and Walter, 1999). To investigate whether Blm10 function is required for this process, we examined rapamycin-induced RP gene repression in the presence or absence of *BLM10*. Rapamycin-induced RP gene down-regulation was significantly attenuated in *blm10*Δ cells (Figure 3D), suggesting that Blm10 is required for correct TORC1-mediated RP gene repression.

The transcription of *BLM10* responds to metabolic changes

Our data suggest a regulatory function of Blm10-mediated proteasomal degradation under nutrient deprivation. We reasoned that this role might be reflected in the transcriptional profile of *BLM10* expression. Proteasome protein levels increase under nutrient deprivation (Fujimuro *et al.*, 1998). Blm10 expression has not been

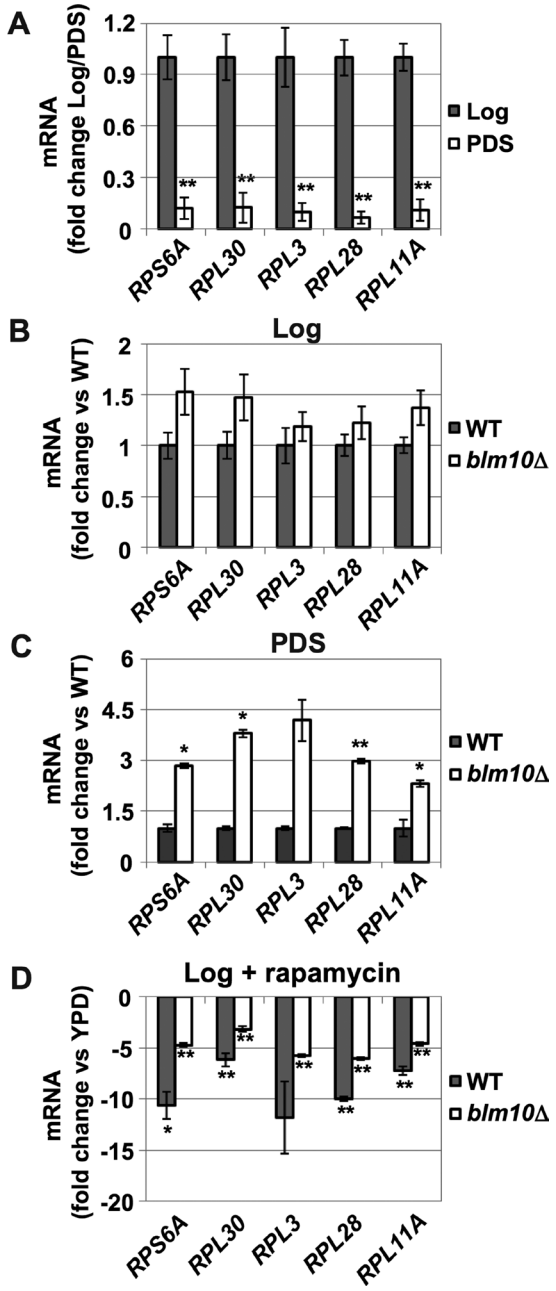

FIGURE 3: RP gene transcription is increased in *BLM10*-deleted cells after the diauxic shift. Expression of RP genes (*RPS6A*, *RPL30*, *RPL3*, *RPL28*, *RPL11*) was analyzed using qRT-PCR. Cycle threshold (C_T) values were normalized to ACT1 expression levels. Data are reported as mean ± SEM. A single asterisk indicates a P-value < 0.05; a double asterisk indicates P < 0.01. (A) RP gene transcription is repressed in PDS. The level of RP gene expression in WT (yMS524) cells was determined in log and PDS phase in four independent experiments. PDS values are normalized to log expression levels. (B and C) Up-regulation of RP gene transcription in *BLM10*-deleted cells in PDS. RP gene transcription was analyzed in WT (yMS524) and *blm10*Δ (yMS63) in log (B) and PDS (C). RP gene expression in *blm10*Δ cells was normalized to WT expression in log or PDS phase. The values represent the mean of three independent experiments. (D) *BLM10*-deleted cells are less responsive to rapamycin-induced RP gene repression. mRNA expression of RP genes was analyzed 1 h after the addition of rapamycin (50 ng/ml) to logarithmically growing WT (yMS524) and *BLM10*-deleted (yMS63) cells in YPD. The values of RP gene expression levels after rapamycin treatment were normalized to the untreated control strains. The values represent the mean of three independent experiments.

investigated so far. We therefore tested the expression of *BLM10*, regulatory particle (*RPN11* and *RPT2*), and CP subunits (*PRE1* and *PRE4*) via qRT-PCR during growth in complete media (Figure 4A). While *BLM10* and proteasome subunit expression remained constant and at a basal level during log growth, expression of all genes tested increased after the diauxic shift (Figure 4B, 10 h and 22 h), that is, when nutrients become limiting.

Rapamycin induces an artificial starvation response even under optimal nutrient conditions. In contrast to the expression of proteasome subunits, *BLM10* mRNA levels were elevated rapidly after 1 h of rapamycin addition (Figure 4C). The latter observation is corroborated by a genome-wide study that analyzed the transcriptional response to rapamycin in yeast. *BLM10* was found to be among the genes most strongly induced by rapamycin (Hardwick *et al*., 1999). Blm10 forms a proteasome subpopulation in log phase (Schmidt *et al*., 2005). Because the expression of proteasomal genes is less responsive to rapamycin, the divergent regulation of proteasome subunits versus *BLM10* expression might indicate a redistribution of proteasome populations during nutrient depletion.

Blm10-proteasomes participate in RP gene repression via degradation of the transcriptional activator Sfp1

We reasoned that the elevated RP mRNA levels upon nutrient depletion in *blm10*Δ cells might originate from inefficient proteasome-mediated elimination of transcriptional activators during nutrient deprivation. Such a model is supported by reports that demonstrate that proteasomes participate in the regulation of transcription through the degradation of transcriptional activators (Lipford and Deshaies, 2003; Collins and Tansey, 2006). An important transcriptional activator for sustained RP gene transcription during logarithmic growth is Sfp1 (Marion *et al*., 2004; Lempiainen *et al*., 2009; Singh and Tyers, 2009). We tested the steady-state levels of Sfp1 in the different metabolic phases in WT cells. A strong reduction of Sfp1 protein levels was apparent in WT cells after the diauxic shift and in stat phase (Figure 5A), indicating that Sfp1 function might be regulated at the protein level. In *blm10*Δ cells increased protein levels of Sfp1 were found in all metabolic phases analyzed as compared with WT (log, PDS, and stat) (Figure 5A), suggesting a function for Blm10 in proteasome-mediated turnover of Sfp1. To rule out that *BLM10* deletion results in elevated *SFP1* transcription, which could explain an increase in Sfp1 abundance, we tested *SFP1* mRNA levels and found them largely unaffected or even reduced by *BLM10* deletion (Figure 5B). Thus the elevated Sfp1 protein levels observed upon *BLM10* deletion are likely caused by a defect in protein turnover. To investigate whether Sfp1 stabilization is a general consequence of proteasome dysfunction, we tested the steady-state level of Sfp1 in the proteasomal ATPase mutant (*rpt3R*; Rubin *et al*., 1998). As with *BLM10* deletion, loss of the ATPase activity of Rpt3 results in elevated Sfp1 levels (Figure 5C).

The CHX-resistant phenotype of *blm10*Δ cells is lost upon *SFP1* deletion

SFP1-deleted cells exhibit a strong growth defect in the presence of low doses of CHX (Fingerman *et al*., 2003), while *BLM10*-deleted cells exhibit CHX resistance (Figures 1A and 5D). To investigate an epistatic relationship between the two genes, we constructed double mutants and tested them for growth on low doses CHX. The growth advantage of *blm10*Δ in the presence of low doses of CHX is lost in the absence of *SFP1* (Figure 5D). Considering the results shown above, we propose that the CHX-resistant phenotype of *BLM10*-deleted cells originates from Sfp1 stabilization.

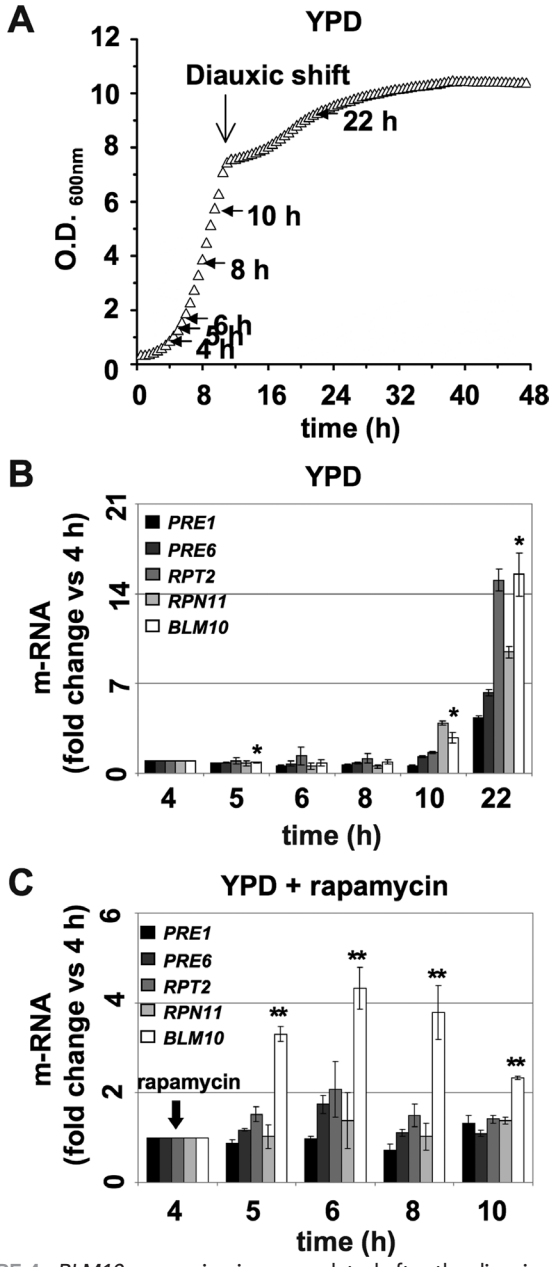

FIGURE 4: *BLM10* expression is up-regulated after the diauxic shift or in the presence of rapamycin. (A) Schematic of cell sampling (marked by arrows) during growth in YPD for the qRT-PCR analysis shown in (B). (B) Expression profile of proteasome subunits and *BLM10* during growth in YPD. mRNA abundance of CP subunits (*PRE1* and *PRE6*), regulatory particle subunits (*RPN11* and *RPT2*), and *BLM10* was analyzed in WT (yMS268) via qRT-PCR at the time points indicated by arrows in (A). C_T values were normalized to ACT1 expression levels. Values for each gene are presented relative to the 4-h time point. Data are reported as mean ± SEM. P-values for Blm10 expression are presented. A single asterisk indicates a P-value < 0.05; a double asterisk indicates P < 0.01. (C) Expression profile of *PRE1*, *PRE6*, *RPN11*, *RPT2*, and *BLM10* in WT cells in the presence of 50 ng/ml rapamycin, which was added at the 4-h time point. Values were obtained as in (B) and at the time points indicated in (A).

Proteasome-mediated Sfp1 degradation requires Blm10

To corroborate that Sfp1 turnover is mediated by proteasomes and is dependent on Blm10, we performed CHX chase experiments (Kornitzer, 2002) in rapidly growing cells. The experimental approach involves lethal doses of CHX, which blocks translation and

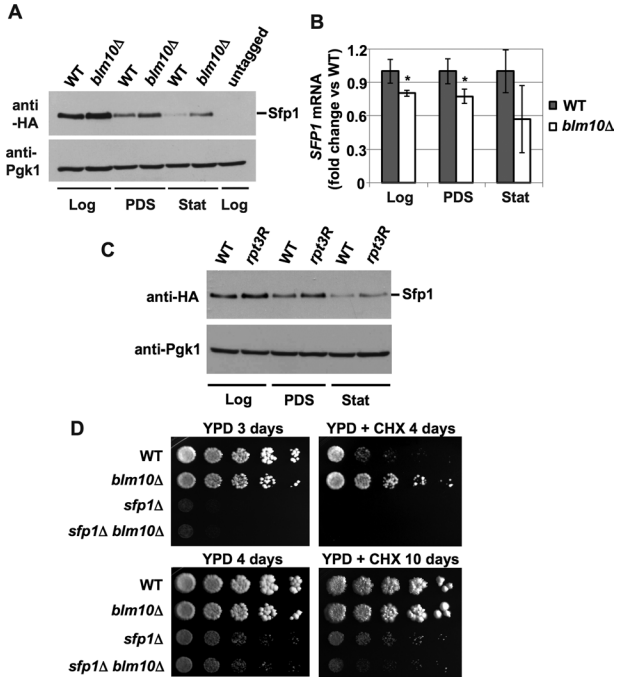

FIGURE 5: Deletion of *BLM10* results in elevated Sfp1 levels. (A) Sfp1 steady-state levels are increased in *BLM10*-deleted cells. *SFP1-HA3* (yMS908) and *SFP1-HA3 blm10*Δ (yMS909) strains were grown to the different metabolic phases in YPD and lysed. Equal protein amounts were separated by SDS–PAGE and subjected to immunodetection with an anti-HA antibody to detect SFP1-HA_3 (top). Pgk1 protein levels were used as a loading control (bottom). (B) *SFP1* transcription is not significantly altered upon loss of *BLM10*. WT (yMS524) and *BLM10*-deleted cells (yMS63) were grown to the different metabolic phases, and *SFP1* mRNA levels were determined via qRT-PCR. C_T values were normalized to *ACT1* expression levels. *SFP1* mRNA levels in *blm10*Δ were normalized to the WT levels. Data are reported as mean ± SEM. A single asterisk indicates a P-value < 0.05; a double asterisk indicates P < 0.01. (C) Sfp1 protein levels are increased in *rpt3R* mutants. WT (yMS1092) and *rpt3R* (yMS1093) were grown to the different metabolic phases and analyzed as in Figure 2B. (D) Epistatic genetic interaction between *BLM10* and *SFP1*. Log phase WT (yMS268), *blm10*Δ (yMS131), *sfp1*Δ (yMS1011), and *sfp1*Δ *blm10*Δ (yMS1012) strains were serially diluted and spotted onto YPD media in the absence (left) or presence of 0.2 μg/ml CHX (right).

cell cycle and results in a growth arrest (McCusker and Haber, 1988; Supplemental Figure 2). In the absence of new synthesis, the half-life of a protein can be determined. We found that in WT cells Sfp1 has a short half-life of ~35 min, indicating continuous turnover of Sfp1 (Figure 6A). In the presence of MG132, a proteasome inhibitor, Sfp1 half-life increased to ~108 min (Figure 6B). Thus Sfp1 degradation is mediated by the proteasome. A similar increase in Sfp1 half-life was detected in *blm10*Δ cells, demonstrating that Sfp1 degradation is executed most likely by Blm10-proteasomes (Figure 6C). Because the addition of MG132 did not increase Sfp1 half-life further in *BLM10*-deleted cells (Figure 6D), our data argue for a model in which Sfp1 degradation might be specifically mediated by Blm10-proteasomes, but not by other proteasome complexes. Although MG132 is readily taken up by yeast cells, it is also rapidly exported from the cell by specific transporters. To investigate the effect of MG132, a *PDR5* deletion strain, a gene that codes for an export pump had to be used (Fleming *et al.*, 2002). To ascertain that the lethal CHX dose used for the chase experiment indeed inhibits cell growth in a *pdr5*Δ strain background, we tested the strains used in Figure 6, A–D, for sensitivity to CHX. The *pdr5*Δ strains are exquisitely sensitive to CHX, independent of the presence or absence of *BLM10* (Supplemental Figure 3).

Blm10 has been implicated in proteasome assembly (Fehlker *et al.*, 2003; Li *et al.*, 2007; Marques *et al.*, 2007). In consequence, impaired Sfp1 turnover could potentially be explained by a general impairment of proteasome structural integrity upon loss of *BLM10*. To compare the proteolytic capacity of proteasomes in WT and *blm10*Δ cells, we tested the turnover of a general proteasome substrate, Ubc6 (Walter *et al.*, 2001; Ravid *et al.*, 2006). Loss of *BLM10* did not influence the turnover of Ubc6 (Figure 7, A and B), whereas deletion of the proteasome-related transcription factor Rpn4, which results in reduced proteasome abundance (Xie and Varshavsky, 2001; Schmidt *et al.*, 2005), effectively inhibited Ubc4 turnover. Thus, in the absence of Blm10, proteasomes are fully functional, arguing against impaired proteasome assembly in *blm10*Δ cells. The result additionally corroborates a model in which Blm10-proteasomes might target a subgroup of proteasome substrates (Schmidt *et al.*, 2005). To

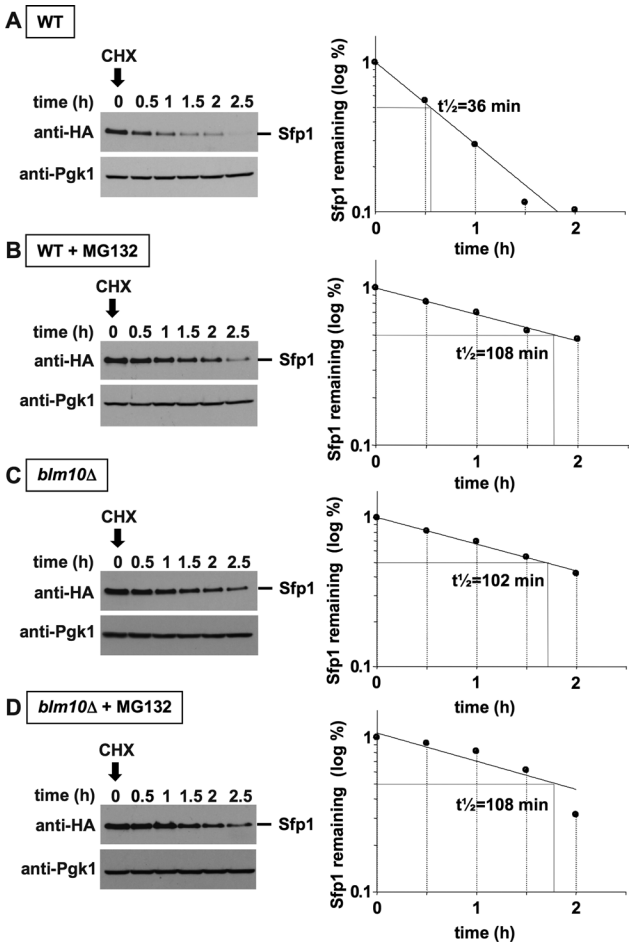

FIGURE 6: Proteasomal degradation of Sfp1 requires the activator Blm10. Logarithmically growing *SFP1-HA pdr5*Δ (yMS957) or *SFP1-HA blm10*Δ *pdr5*Δ (yMS958) cells were grown in the absence (A and C) or presence of the proteasome inhibitor MG132 (B and D) for 3 h at 30°C. Subsequently, translation was blocked with 200 μg/ml CHX, and aliquots were harvested and processed at the time points indicated. Equal amounts of protein were subjected to SDS–PAGE, followed by immunodetection with an HA-specific antibody to detect Sfp1 protein levels (left). Pgk1 immunodetection was used as a loading control (bottom). A densitometric analysis of the Sfp1 protein levels is depicted on the right. Sfp1 half-life (t½) was calculated from an exponential decay curve with SigmaPlot 11.0.

further investigate the interaction between Sfp1 and Blm10-proteasomes, we mapped their physical interaction by CP immunoprecipitation (Figure 7D, right) in the absence or presence of *BLM10*. We found that Sfp1 copurifies with the proteasome in both WT and *blm10*Δ cells, indicating that Sfp1 interaction with the proteasome is not mediated by direct interaction of Sfp1 with Blm10. However, in *blm10*Δ cells the Sfp1 protein level, which copurified with the CP, was elevated, demonstrating that Blm10 positively affects the regulated turnover of Sfp1 at the proteasome.

Loss of *BLM10* leads to increased ribosome function

It is well established that changes in Sfp1 levels affect ribosome abundance. The *sfp1*Δ cells show reduced levels of 80S ribosomes and higher-order polyribosomes compared with WT cells (Fingerman *et al.*, 2003), while elevated Sfp1 level results in increased transcription of RP genes (Jorgensen *et al.*, 2004). To test whether the elevated RP levels we observed upon Sfp1 stabilization in the absence of *BLM10* lead to an increase in functional ribosomes, we compared the sucrose gradient profiles of ribosomal subunits and polyribosomes in WT, *blm10*Δ, *sfp1*Δ, and *SFP1*– overexpressing cells. Loss of *SFP1* results in a reduced pool of 80S ribosomes and higher-order polyribosomes (Figure 8C), as previously described (Fingerman *et al.*, 2003). Cells overexpressing *SFP1*, on the other hand, exhibit increased 80S ribosomes and polyribosomes. Consistent with the data reported above, *BLM10* deletion results in a profile similar to *SFP1* overexpression (Figure 8B).

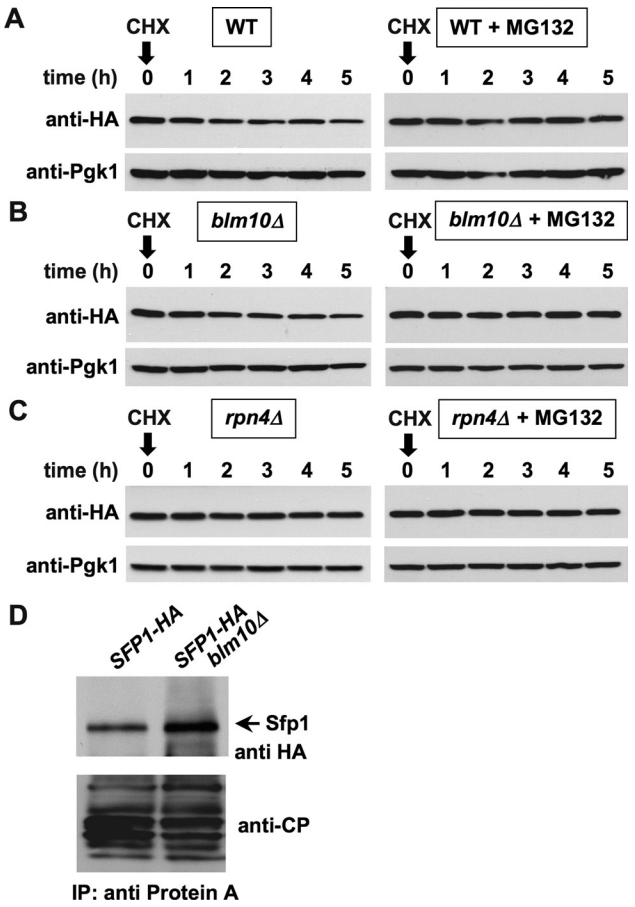

FIGURE 7: Loss of *BLM10* does not lead to a general impairment of proteasome function (A and B). Turnover of the proteasome substrate Ubc6 was determined in WT (*UBC6-HA*$_3$ *pdr5*Δ [yMS792]) or in *blm10*Δ (*UBC6-HA*$_3$ *blm10*Δ *pdr5*Δ [yMS1089]). (C) Ubc6 is stabilized in *rpn4*Δ cells. Turnover of the proteasome substrate Ubc6 in *rpn4*Δ (*UBC6-HA*$_3$ *rpn4*Δ *pdr5*Δ [yMS1364]) strain. Pgk1 immunodetection was used as a loading control (bottom). (D) Sfp1 interacts with Blm10-proteasomes. For CP pull-down cells from yMS1189 and from yMS1190 containing protein A–tagged Pre1 and carrying SFP1–HA$_3$ in the presence (yMS1189) or in the absence (yMS1190) of *BLM10* were harvested in logarithmic (log) phase, lysed, and subjected to immune precipitation. The samples were separated by SDS–PAGE and probed with anti-HA (top) or anti-CP (bottom) antibodies.

Sfp1 accumulates in the nucleus in *BLM10*-deleted cells

Sfp1 function appears to be controlled by differential localization. While the protein is localized predominantly to the nucleus if nutrients are abundant, it is found evenly distributed in the cell after the diauxic shift or upon rapamycin treatment (Jorgensen *et al.*, 2004; Marion *et al.*, 2004). A current model for the repression of RP gene transcription under nutrient-limiting conditions involves the dissociation of Sfp1 from RP gene promoters, followed by nuclear export of the protein. We demonstrate here that Sfp1 is degraded after the diauxic shift, and if degradation is abrogated due to loss of Blm10 or upon proteasome inhibition, the protein is stabilized and the repression of RP gene transcription is attenuated. The higher levels of RP mRNA in *blm10*Δ cells suggest that a significant fraction of Sfp1 must remain functional and bound to RP gene promoters even under repressive conditions. To test Sfp1 localization in *BLM10*-deleted cells, we tagged the C-terminus of Sfp1 with green fluorescent protein (GFP) and performed live-cell fluorescence microscopy. As reported previously in WT cells (Marion *et al.*, 2004; Lempiainen *et al.*, 2009; Singh and Tyers, 2009), the predominant nuclear localization of Sfp1 during log growth (Figure 9A, top) is lost in PDS (Figure 9B, top). In *blm10*Δ log phase cells, Sfp1 is also detected predominantly in the nucleus (Figure 9A, bottom). In PDS, however, loss of *BLM10* results in a high fraction of Sfp1 retained in the nucleus (Figure 9B, bottom, and 9C). The higher Sfp1 levels in *blm10*Δ cells after the diauxic shift are also reflected in increased intensity of Sfp1-GFP fluorescence if the cells are imaged with identical exposure times (Supplemental Figure 4).

DISCUSSION

Nutrient depletion in *S. cerevisiae* results in a rapid cellular response characterized by a metabolic switch from fermentation to oxidative metabolism (Herman, 2002). The major targets of this metabolic

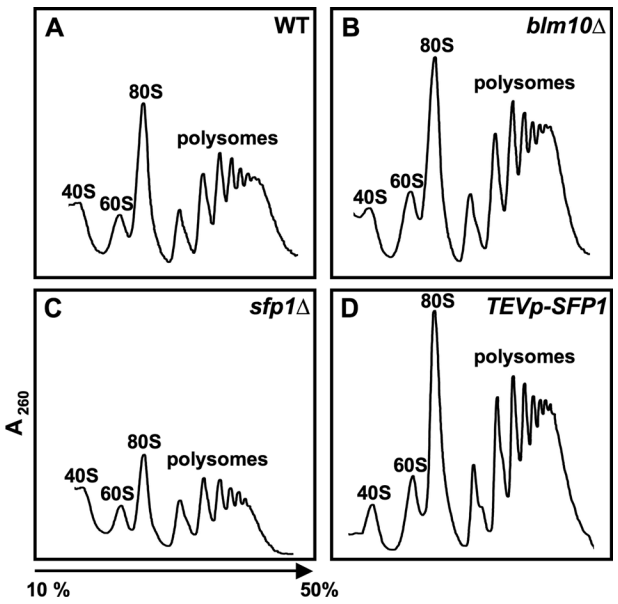

FIGURE 8: Polyribosome profiles of cells with varying Sfp1 levels. Polyribosomes profiles were recorded for WT (A), *blm10*Δ (B), *sfp1*Δ (C), and SFP1–overexpressing cells (*TEVpSFP1*) (D).

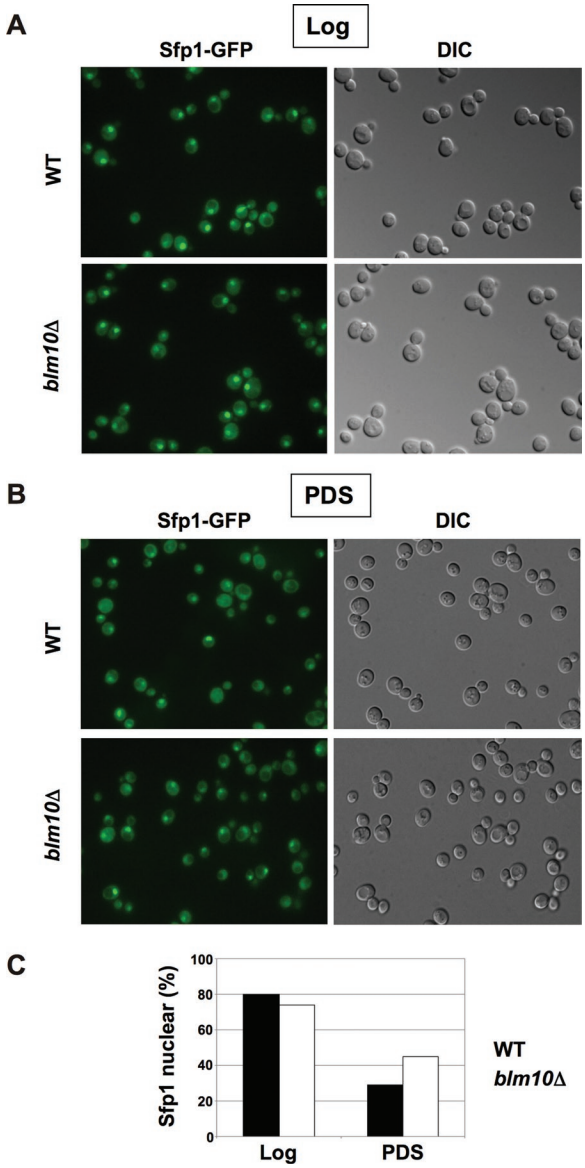

FIGURE 9: Impaired Sfp1 localization in *BLM10*-deleted cells after the diauxic shift. (A) *SFP1-GFP* (yMS928) and *SFP1-GFP blm10*Δ (yMS929) cells were grown in synthetic complete media. Sfp1 localization was visualized in log phase via live-cell fluorescence. Differential interference contrast (DIC) images are shown on the right. (B) Sfp1 localization in PDS phase cells was analyzed in *SFP1-GFP* (yMS928) and *SFP1-GFP blm10*Δ (yMS929) as in (A). (C) Quantification of cells with nuclear Sfp1 localization in log and PDS in WT (yMS928) and *blm10*Δ (yMS929) from 10 independent fluorescent micrographs with ~500 cells each, using ImageJ software 1.42q for visualization.

adaptation are the mitochondria and the ribosomes. While mitochondrial activity is induced after the diauxic shift to improve the efficiency of ATP generation, ribosome biogenesis and function are down-regulated due to the high energy investment in ribosome synthesis and translation (Warner, 1999). Ribosome synthesis requires the expression of three tightly regulated gene clusters: the rRNA genes, the 137 RP genes, and the >200 ribosome biogenesis (Ribi) genes (Jorgensen *et al.*, 2004; Wade *et al.*, 2004). After the diauxic shift, the transcription of these genes is rapidly repressed (Brauer *et al.*, 2005).

In *S. cerevisiae* the machinery that activates ribosomal gene transcription involves several transcription factors and activators. The repression of ribosomal gene transcription is less well understood. Recent findings indicate that differential localization of Sfp1 mediates the repression of RP genes (Lempiainen *et al.*, 2009; Singh and Tyers, 2009). Sfp1 is a split-zinc finger transcription factor, which might represent the functional analog of c-Myc in yeast (Jorgensen *et al.*, 2004). It was identified as a factor that strongly influences cell size and growth. The underlying reason for the small-cell-size phenotype of *sfp1*Δ cells is improper regulation of RP and Ribi gene expression (Marion *et al.*, 2004). Under favorable nutrient conditions, Sfp1 is localized to the nucleus and binds to RP gene promoters (Marion *et al.*, 2004; Lempiainen *et al.*, 2009; Singh and Tyers, 2009). Nutrient depletion results in its relocalization to the cytoplasm. Mutations in putative Sfp1 TORC1 phosphorylation sites partially abrogate its nuclear localization (Lempiainen *et al.*, 2009), and nuclear accumulation of Sfp1 is prevented in the presence of rapamycin (Marion *et al.*, 2004; Singh and Tyers, 2009). Thus TORC1-dependent phosphorylation is thought to mediate localization and promoter binding of Sfp1. As loss of *SFP1* results in the mislocalization of two other critical factors for RP gene transcription, Fhl1 and Ifh1 (Jorgensen *et al.*, 2004), Sfp1 function and localization appear to play a central role in the regulation of RP gene transcription.

Here we report that in rapidly growing cells Sfp1 has a short half-life of ~38 min. Sfp1 turnover is impeded by proteasome inhibition or upon loss of the proteasome activator Blm10. Thus Sfp1 levels are regulated by proteasomal degradation in a process that is mediated by Blm10. Loss of *BLM10* results in increased RP gene transcription, increased RP levels, increased abundance of active ribosomes, and resistance to low doses of CHX. Furthermore, *blm10*Δ cells exhibit increased nuclear abundance of Sfp1 during nutrient depletion, suggesting that nuclear export of Sfp1 per se is not sufficient to terminate its function. In summary, our results argue for a functional participation of proteasomes in the repression of ribosome biogenesis during nutrient depletion through degradation of Sfp1. Interestingly, proteasome recruitment to RP genes has been demonstrated recently (Auld *et al.*, 2006). It is therefore tempting to speculate that Sfp1 turnover might occur at the actively transcribed gene, potentially to remove transcriptional complexes after transcription initiation or during the termination of transcription.

The proteasome has different functions in eukaryotic cells: 1) clearance of abnormal proteins to avoid proteotoxicity, 2) a metabolic function by providing building blocks for protein synthesis under starvation conditions, and 3) a regulatory signaling function exerted by the temporally controlled elimination of specific proteins. Ribosomes and proteasomes represent two macromolecular complexes with opposite functions to maintain proteostasis. Thus it could be expected that the first two functions largely determine the relationship between both complexes. Indeed, the proteasome degrades defective ribosomal products (DRiPs) and thus prevents the accumulation of damaged proteins produced by the ribosome (Schubert *et al.*, 2000). Proteasome levels are also up-regulated under starvation conditions to supply amino acids for protein synthesis (Lecker *et al.*, 2006). However, there is increasing evidence that proteasomes also exhibit regulatory functions during ribosome biogenesis. In genome-wide analyses in *S. cerevisiae*, proteasome subunits were detected at promoters of highly transcribed genes in general, and of RP genes in particular (Auld *et al.*, 2006). Heterozygous proteasomal gene deletions result in a large cell phenotype indicative of increased ribosome function (Jorgensen *et al.*, 2004), which in the light of the present study is most likely caused by impaired Sfp1 degradation. Furthermore, proteasome inhibition in mammalian cells revealed dysregulated ribosome maturation such as the accumulation of 90S preribosomes and altered nucleolar morphology (Stavreva *et al.*, 2006). A significant portion of RPs is

degraded by the proteasome before ribosome formation in mammalian cells (Lam *et al.*, 2007). Proteasome-mediated degradation of Sfp1, as reported in this study, adds an additional layer to the complex interaction between the proteasome and ribosome biogenesis and function by providing a regulatory mechanism for the repression of RP gene transcription under nutrient limitation.

The precise impact of Blm10 on proteasome function is unknown. Previous reports suggest that Blm10 might play a role in proteasome assembly (Fehlker *et al.*, 2003) and thus might represent a proteasome chaperone required for correct proteasome biogenesis. Several lines of evidence, however, point to a function beyond maturation. 1) *blm10*Δ cells do not exhibit assembly defects (Marques *et al.*, 2007). 2) In contrast to the nine identified proteasome assembly chaperones, which either dissociate or are degraded after correct structure formation (Bedford *et al.*, 2010), Blm10 copurifies with mature proteasomes and forms a stable proteasome subpopulation (Schmidt *et al.*, 2005; Lehmann *et al.*, 2008). 3) Different from proteasome chaperones, Blm10 binds to the CP gate region, a critical regulatory entry point for proteasome substrates (Schmidt *et al.*, 2005; Iwanczyk *et al.*, 2006) 4) On Blm10 binding, the CP gate region undergoes structural changes resulting in partial gate opening, as evident from the $Blm10_2$–CP crystal structure (Sadre-Bazzaz *et al.*, 2010). 5) Blm10 activates the proteasomal peptidase activity (Schmidt *et al.*, 2005; Iwanczyk *et al.*, 2006; Lehmann *et al.*, 2008; Sadre-Bazzaz *et al.*, 2010). These observations are in line with typical characteristics of proteasome activators, such as the RP or the PA28 activator family.

The data reported here provide additional support for a potential proteasome activator function of Blm10 and suggest that Blm10 promotes the degradation of specific proteasome substrates. Loss of *BLM10* results in the stabilization of Sfp1. Furthermore, treatment of *blm10*Δ cells with proteasome inhibitors does not result in additional stabilization of Sfp1, arguing for a Blm10-proteasome–specific mechanism. In contrast, turnover of the proteasome substrate Ubc6 is unaffected by loss of *BLM10*, while Ubc6 is stabilized in *rpn4*Δ cells, which are characterized by low proteasome levels. These findings argue for fully functional proteasomes in the absence of Blm10 and against a major role of Blm10 in proteasome assembly.

If Blm10 functions as an activator for proteasomal protein degradation, then the interaction between Blm10 and the CP should involve opening of the CP gate. Indeed, an open or partially open gate has been observed in $Blm10_2$–CP cryo-electron microscopy and crystal structures (Iwanczyk *et al.*, 2006; Sadre-Bazzaz *et al.*, 2010). Previous studies suggest two distinct gate-opening mechanisms. C-terminal docking of PA26 is not sufficient for gate opening but requires a second internal loop structure. The C-termini of the RP ATPases, on the other hand, directly structurally alter the gate region to promote gate opening (Rabl *et al.*, 2008). The cocrystal structure of $Blm10_2$–CP suggests that Blm10 C-terminal docking has similar consequences at the molecular level for gating as binding of the proteasomal ATPases (Sadre-Bazzaz *et al.*, 2010). Thus alterations within the Blm10 C-terminus might result in disrupted binding or gating, and C-terminal mutants might exhibit a loss-of-function phenotype. We addressed this hypothesis with a phenotypic characterization of Blm10 C-terminal mutants. They fall in two classes. C-terminal mutants, which abrogate CP binding (*BLM10*Δ*C2* and *BLM10*Δ*C3*), exhibit a loss-of-function phenotype (CHX resistance), indicating that proteasomal degradation of Sfp1 requires physical interaction of Blm10 with the CP. The second class of C-terminal mutants (*BLM10*Δ*C1* and *BLM10PA26C*) is proteasome-binding competent yet displays CHX resistance. Although we cannot exclude alternative scenarios, we speculate that the loss-of-function phenotype of both mutants, especially the *BLM10PA26C* chimera, where the last seven residues have been exchanged against the gating-inactive C-terminal residues of PA26, might reflect impaired gate opening of these Blm10 mutants and thus impaired Sfp1 turnover. In summary, our data provide the first evidence indicating that the physical interaction of Blm10 with the proteasomes might promote the degradation of specific proteasome substrates.

MATERIALS AND METHODS

Strains, media, growth conditions, and chemicals

All strains and plasmids used in this work are listed in Table 1. They were obtained using standard genetic techniques. Unless otherwise noted, strains are isogenic to BY4741 or BY4742 (Brachmann *et al.*, 1998) and are S288C derived. DY93 and DY106 and their parental strain SUB62 were kind gifts from Daniel Finley (Rubin *et al.*, 1998). Complete gene deletion, promoter exchange, or tag integration were constructed at the genomic locus by homologous recombination using standard techniques (Longtine *et al.*, 1998; Goldstein and McCusker, 1999). Primer sequences are available upon request. Unless otherwise noted, strains were grown at 30°C in yeast peptone dextrose (YPD) and were harvested at $OD_{660\,nm}$ 1 for log phase cells, at $OD_{660\,nm}$ ~12 for PDS phase cells, and after 5 d for stat phase cells unless otherwise noted. CHX was purchased from Sigma (St. Louis, MO), hygromycin B from Invitrogen (Carlsbad, CA), rapamycin from A. G. Scientific (San Diego, CA), MG132 from Calbiochem (Darmstadt, Germany), and *N*-succinyl-Leu-Leu-Val-Tyr-7-amino-4-methylcoumarin (Suc-LLVY-AMC) from Bachem (Torrance, CA).

Blm10-proteasome purification and in situ assay to determine CP peptidase activity

For the purification of WT and mutant Blm10–CP complexes, cells from yMS31, yMS568, yMS569, yMS570, and yMS573 containing protein A–tagged Pre1 were collected and lysed using French press cell disruption. Purification was performed as described previously (Schmidt *et al.*, 2005). Briefly, the cleared lysate was batch incubated with IgG Affinity gel (MP Biomedicals, Solon, OH), and the beads were collected and washed. Proteasome complexes were eluted with tobacco etch virus (TEV) protease (Invitrogen, Carlsbad, CA). Subsequently, the purified complexes were first resolved on 3.5% acrylamide native gels (Schmidt *et al.*, 2005), followed by an in-gel activity assay with the fluorogenic proteasome substrate Suc-LLVY-AMC as described previously and silver staining of the gel (Schmidt *et al.*, 2005).

Phenotypic analysis of gene deletion

Strains were grown overnight in YPD and diluted in 96-well plates to a density of 6×10^6 cells per well followed by fivefold serial dilutions. They were spotted onto YPD plates in the absence or presence of CHX or hygromycin B. The concentration is indicated in the respective figure legend.

Growth curves

Cultures were inoculated overnight in YPD. In the morning the culture was diluted to an $OD_{660\,nm} = 0.1$. Subsequently, four aliquots of 150 µl of the culture were added to an HC2 plate. Growth was recorded in a Bioscreen C MB machine (Growth Curves USA, Piscataway, NJ) for 48 h at 30°C under continuous shaking and with absorbance readings at 600 nm every 30 min.

Immunoprecipitation

For the proteasome CP pull-down cells (strains yMS1189, yMS1190, and untagged control BY4742) were harvested in log

Strain	Genotype	Source
SUB62	Mat**a** *lys2–801 leu2–3, 2–112 ura3–52 his3-Δ200 trp1-1(am)*	Finley *et al.*, 1994
BY4741	Mat**a** *his3Δ1 leu2Δ0 met15Δ0 ura3Δ0*	Brachmann *et al.*, 1998
BY4742	Matα *his3Δ1 leu2Δ0 lys2Δ0 ura3Δ0*	Brachmann *et al.*, 1998
DY106	Mat**a** *lys2–801 leu2–3, 2–112 ura3–52 his3-Δ200 trp1-1(am) rpt1K256S*	Rubin *et al.*, 1998
DY62	Mat**a** lys2–801 *leu2–3, 2–112 ura3–52 his3-Δ200 trp1-1(am) rpt2K229RS241F*	Rubin *et al.*, 1998
DY93	Mat**a** lys2–801 *leu2–3, 2–112 ura3–52 his3-Δ200 trp1-1(am) rpt3K219R*	Rubin *et al.*, 1998
yMS31	Mat**a** *his3Δ1 leu2Δ0 met15Δ0 ura3Δ0 PRE1$_{TEV}$PROA::HIS3*	Schmidt *et al.*, 2005
yMS63	Mat**a** *his3Δ1 leu2Δ0 met15Δ0 ura3Δ0 blm10**Δ**::natMX*	Schmidt *et al.*, 2005
yMS94	Matα *his3Δ1 leu2Δ0 met15Δ0 ura3Δ0 PRE1$_{TEV}$PROA::HIS3 blm10**Δ**::natMX*	Schmidt *et al.*, 2005
yMS131	Matα *his3Δ1 leu2Δ0 met15Δ0 ura3Δ0 blm10**Δ**::natMX*	This study
yMS222	Mat**a** *his3Δ1 leu2Δ0 met15Δ0 ura3Δ0 ubp6**Δ**::KanMX*	This study
yMS268	Matα *his3Δ1 leu2Δ0 met15Δ0 ura3**Δ**0*	This study
yMS524	Mat**a** *his3Δ1 leu2Δ0 lys2Δ0 ura3Δ0*	This study
yMS565	Mat**a** *his3Δ1 leu2Δ0 met15Δ0 ura3Δ0 BLM10**Δ**C1::KanMX*	This study
yMS566	Mat**a** *his3Δ1 leu2Δ0 met15Δ0 ura3Δ0 BLM10**Δ**C2::KanMX*	This study
yMS567	Mat**a** *his3Δ1 leu2Δ0 met15Δ0 ura3Δ0 BLM10**Δ**C3::KanMX*	This study
yMS568	Mat**a** *his3Δ1 leu2Δ0 met15Δ0 ura3Δ0 PRE1$_{TEV}$PROA::HIS3 BLM10**Δ**C1::KanMX*	This study
yMS569	Mat**a** *his3Δ1 leu2Δ0 met15Δ0 ura3Δ0 PRE1$_{TEV}$PROA::HIS3 BLM10**Δ**C2::KanMX*	This study
yMS570	Mat**a** *his3Δ1 leu2Δ0 met15Δ0 ura3Δ0 PRE1$_{TEV}$PROA::HIS3 BLM10**Δ**C3::KanMX*	This study
yMS573	Mat**a** *his3Δ1 leu2Δ0 met15Δ0 ura3Δ0 PRE1$_{TEV}$PROA::HIS3 BLM10PA26C::KanMX*	This study
yMS598	Mat**a** *his3Δ1 leu2Δ0 met15Δ0 ura3Δ0 BLM10PA26C::KanMX*	This study
yMS792	Mat**a** *his3Δ1 leu2Δ0* lys2Δ0 *ura3Δ0 UBC6-HA3::KanMX pdr5**Δ**::HphMX*	This study
yMS908	Mat**a** *his3Δ1 leu2Δ0* lys2Δ0 *ura3Δ0 SFP1-HA3::KanMX*	This study
yMS909	Mat**a** *his3Δ1 leu2Δ0 met15Δ0 ura3Δ0 SFP1-HA3::KanMX blm10**Δ**::natMX*	This study
yMS928	Matα *his3Δ1 leu2Δ0 met15Δ0 ura3Δ0 SFP1-GFP::KanMX*	This study
yMS929	Matα *his3Δ1 leu2Δ0 met15Δ0 ura3Δ0 SFP1-GFP::KanMX blm10**Δ**::natMX*	This study
yMS957	Mat**a** *his3Δ1 leu2Δ0* lys2Δ0 *ura3Δ0 SFP1-HA3::KanMX pdr5**Δ**::HphMX*	This study
yMS958	Mat**a** *his3Δ1 leu2Δ0 met15Δ0 ura3Δ0 SFP1-HA3::KanMX blm10**Δ**::natMX pdr5Δ::HphMX*	This study
yMS1011	Matα *his3Δ1 leu2Δ0 met15Δ0 ura3Δ0 sfp1**Δ**::KanMX*	This study
yMS1012	Matα *his3Δ1 leu2Δ0 met15Δ0 ura3Δ0 sfp1**Δ**::KanMX blm10**Δ**::natMX*	This study
yMS1013	Mat**a** *his3Δ1 leu2Δ0 met15Δ0 ura3Δ0 sfp1**Δ**::KanMX*	This study
yMS1089	Mat**a** *his3Δ1 leu2Δ0 met15Δ0 ura3Δ0 UBC6-HA3::KanMX pdr5**Δ**::HphMX blm10**Δ**::natMX*	This study
yMS1090	Mat**a** *his3Δ1 leu2Δ0 lys2Δ0 ura3Δ0 kanMX::TEVpSFP1*	This study
yMS1092	Mat**a** *lys2–801 leu2–3, 2–112 ura3–52 his3-**Δ**200 trp1-1(am) SFP1-HA3::KanMX*	This study
yMS1093	Mat**a** *lys2–801 leu2–3, 2–112 ura3–52 his3-**Δ**200 trp1-1(am) rpt3K219R SFP1-HA3::KanMX*	This study
yMS1189	Matα *his3Δ1 leu2Δ0 lys2Δ0 ura3Δ0 SFP1-HA3::KanMX PRE1$_{TEV}$PROA::His3*	This study
yMS1190	Matα *his3Δ1 leu2Δ0 ura3Δ0 SFP1-HA3::KanMX PRE1$_{TEV}$PROA::His3 blm10**Δ**::natMX*	This study
yMS1364	Mat**a** *his3Δ1 leu2Δ0 lys2Δ0 ura3Δ0 UBC6-HA3::KanMX pdr5**Δ**::HphMX rpn4**Δ**::natMX*	This study

TABLE 1: Strains used in this study.

phase, resuspended in lysis buffer (50 mM Tris, pH 8, 50 mM NaCl, 5 mM $MgCl_2$, 1 mM EDTA) supplemented with protease inhibitor cocktail (complete, Roche, Indianapolis, IN), 10 mg/ml pepstatin A and 1 mg/ml antipain, and drop-frozen in liquid nitrogen. Frozen yeast cells were lysed in an MM301 grinding mill (Retsch, Haan, Germany) following the manufacturer's protocol. Cell extracts were cleared at 11,000 rpm for 30 min at 4°C and filtered through cheesecloth (VWR International, San Diego, CA). The supernatants were mixed with rabbit immunoglobulin G resin (MP Biomedicals, Solon, OH) and incubated for 2 h at 4°C. The resin was collected at 500 rpm for 2 min at 4°C and washed five times with cold lysis buffer, resuspended in 2× Laemmli sample buffer, and boiled for 5 min, and the supernatants were collected by centrifugation (500 rpm, 3 min). The proteins were separated

by SDS–PAGE, followed by immunodetection for Sfp1-HA and for CP.

Gel electrophoresis and immunoblotting

Cells from WT and mutant strains were harvested in the respective growth phases and stored at −80°C. Cells were disrupted by alkaline lysis as described previously (Kushnirov, 2000). Protein concentration was determined using a Bradford protein assay (Bio-rad, Hercules, CA). Equal protein amounts were subjected to SDS–PAGE and immunodetection. Antibodies used were anti-CP (BIOMOL, Plymouth Meeting, PA), anti-Rpl3, and anti-Rpl30, kindly provided by Jonathan Warner, and anti-HA 12C5 (Roche, Indianapolis, IN). Anti–phosphoglycerate kinase 1 (Pgk1) (Invitrogen, Carlsbad, CA) was used as a loading control. Signals were detected via enhanced chemiluminescence using a kit (Pierce, Rockford, IL).

Protein degradation assay (CHX chase)

Protein turnover was determined using a CHX chase assay (Ravid *et al.*, 2006). To analyze proteasome-dependent degradation, log phase cultures were supplemented with 40 μM for Sfp1 and 75 μM for Ubc6 of MG132 or vehicle (dimethyl sulfoxide [DMSO]) for 3 h or 30 min, respectively, at 30°C before the addition of 0.2 mg/ml CHX. Aliquots were harvested at the times indicated and either immediately frozen at −20°C (Figure 6) or lysed directly (Figure 7). After alkaline lysis (Kushnirov, 2000), equal protein amounts were subjected to SDS–PAGE and immunodetection using an anti-HA antibody to detect Sfp1 or Ubc6 levels. The immunoblots were scanned and band intensity was quantified using ImageJ 1.42q.

qRT-PCR

Total RNA was isolated after an enzymatic digest of the outer cell wall with zymolase (Seikagaku, Tokyo, Japan) using the RNeasy kit (Qiagen, Valencia, CA) according to the manufacturer's protocol. Subsequently, 1 μg RNA was treated with DNAse (Invitrogen), followed by reverse transcription using the High Capacity cDNA kit (Applied Biosystems, Carslbad, CA). TaqMan primers and probes were designed using the software Primer3Plus (Untergasser *et al.*, 2007). The sequences are available upon request. In an Applied Biosystems 7900HT instrument, 5 ng cDNA was subjected to qRT-PCR. The reactions were performed in 40 cycles of a two-step PCR (95°C for 15 s and 60°C for 1 min) after an initial activation with 50°C for 2 min and 95°C for 10 min. Negative controls were run simultaneously for each reaction. Data were analyzed using ABI Prism 7900 SDS 2.1v (Applied Biosystems) software. To compare the relative mRNA expression between the individual genes and the endogenous reference gene *ACT1*, the comparative threshold cycle (C_T) method was used. The amount of target, relative to the reference gene as described in the individual figure legends, is given by $2^{-}\Delta\Delta^{C}{}_{T}$. All reactions were performed in quadruplicates. Error bars indicate the mean ± SEM of at least three independent experiments. Statistical significance of the obtained data was determined with the independent-samples *t*-test analysis using SPSS version 16 software (SPSS, Chicago, IL). P-values < 0.05 were considered statistically significant.

Polyribosome profile analysis

For polyribosome preparation, 50 ml cultures of BY4741, yMS63, yMS1013, and yMS1090 were grown to log phase (OD_{660} 0.8–1.0), and CHX was added to a final concentration of 100 μg/ml. The cells were chilled immediately on ice. After centrifugation at 5000 rpm for 5 min at 4°C, the cell pellets were washed once with 10 ml ice-cold LHB buffer (0.1 M NaCl, 0.03 M $MgCl_2$, 0.01 M Tris, pH 7.4, 100 μg/ml CHX, 200 μg/ml heparin) and resuspended in 0.5 ml cold LHB buffer. A 700-μl volume of glass beads was added, and the cells were vortexed 1 × 1 min in a BeadBeater. The lysates were spun down briefly to reduce foam and diluted with LHB to a final volume of 1.5 ml. After centrifugation in a microcentrifuge for 10 min at maximum speed and 4°C, A_{260} was measured, and 10 OD_{260} units were loaded onto a sucrose gradient (11 ml 10–50% sucrose in 0.05 M Tris-Ac, pH 7.0, 0.05 M NH_4Cl, 0.012 M $MgCl_2$). The gradients were centrifuged in a Beckman SW41 rotor at 40,000 rpm for 2.5 h, and A_{260} of gradient fractions was read using an ISCO UA-5 absorbance detector.

Microscopy

yMS928 and yMS929 carrying C-terminally GFP-tagged Sfp1 were grown overnight in synthetic dextrose at 30°C to PDS. Cells were either rediluted in the morning to an $OD_{660\ nm}$ 0.1 and grown for additional 3 h to obtain log phase cultures or were harvested immediately. Live-cell fluorescence of the strains was monitored using a fluorescence microscope (Olympus BX61) at the Albert Einstein Imaging Facility with a 60× NA 1.4 objective (PlanApo). Fluorescence or differential interference contrast (DIC) images were captured with a cooled CCD camera (Sensicam QE, Cooke, Romulus, MI) using IPlab 4.0 software. Images were processed using ImageJ software 1.42q.

ACKNOWLEDGMENTS

We thank Jonathan Warner for providing us with antibodies and access to the Bioscreen C MB instrument, Kerri Macintosh for support with the polyribosome profiles, Daniel Finley for yeast mutant strains, and Philip Rommel for technical support. This work was supported by grants from the National Institute of Health GM-084228 to MS and a fellowship from the Spanish Ministerio de Ciencia e Innovación to ADL.

REFERENCES

Auld KL, Brown CR, Casolari JM, Komili S, Silver PA (2006). Genomic association of the proteasome demonstrates overlapping gene regulatory activity with transcription factor substrates. Mol Cell 21, 861–871.

Bedford L, Paine S, Sheppard PW, Mayer RJ, Roelofs J (2010). Assembly, structure, and function of the 26S proteasome. Trends Cell Biol 20, 391–401.

Berger AB, Decourty L, Badis G, Nehrbass U, Jacquier A, Gadal O (2007). Hmo1 is required for TOR-dependent regulation of ribosomal protein gene transcription. Mol Cell Biol 27, 8015–8026.

Blickwedehl J, Agarwal M, Seong C, Pandita RK, Melendy T, Sung P, Pandita TK, Bangia N (2008). Role for proteasome activator PA200 and postglutamyl proteasome activity in genomic stability. Proc Natl Acad Sci USA 105, 16165–16170.

Brachmann CB, Davies A, Cost GJ, Caputo E, Li J, Hieter P, Boeke JD (1998). Designer deletion strains derived from *S. cerevisiae* S288C: a useful set of strains and plasmids for PCR-mediated gene disruption and other applications. Yeast 14, 115–132.

Brauer MJ, Saldanha AJ, Dolinski K, Botstein D (2005). Homeostatic adjustment and metabolic remodeling in glucose-limited yeast cultures. Mol Biol Cell 16, 2503–2517.

Claypool JA, French SL, Johzuka K, Eliason K, Vu L, Dodd JA, Beyer AL, Nomura M (2004). Tor pathway regulates Rrn3p-dependent recruitment of yeast RNA polymerase I to the promoter but does not participate in alteration of the number of active genes. Mol Biol Cell 15, 946–956.

Collins GA, Tansey WP (2006). The proteasome: a utility tool for transcription? Curr Opin Genet Dev 16, 197–202.

Febres DE, Pramanik A, Caton M, Doherty K, McKoy J, Garcia E, Alejo W, Moore CW (2001). The novel BLM3 gene encodes a protein that protects against lethal effects of oxidative damage. Cell Mol Biol (Noisy-le-grand) 47, 1149–1162.

Fehlker M, Wendler P, Lehmann A, Enenkel C (2003). Blm3 is part of nascent proteasomes and is involved in a late stage of nuclear proteasome assembly. EMBO Rep 4, 959–963.
Fingerman I, Nagaraj V, Norris D, Vershon AK (2003). Sfp1 plays a key role in yeast ribosome biogenesis. Eukaryot Cell 2, 1061–1068.
Finley D (2009). Recognition and processing of ubiquitin-protein conjugates by the proteasome. Annu Rev Biochem 78, 477–513.
Finley D, Sadis S, Monia BP, Boucher P, Ecker DJ, Crooke ST, Chau V (1994). Inhibition of proteolysis and cell cycle progression in a multiubiquitination-deficient yeast mutant. Mol Cell Biol 14, 5501–5509.
Fleming JA, Lightcap ES, Sadis S, Thoroddsen V, Bulawa CE, Blackman RK (2002). Complementary whole-genome technologies reveal the cellular response to proteasome inhibition by PS-341. Proc Natl Acad Sci USA 99, 1461–1466.
Foerster A, Whitby FG, Hill CP (2003). The pore of activated 20S proteasomes has an ordered 7-fold symmetric conformation. EMBO J 22, 4356–4364.
Fujimuro M, Takada H, Saeki Y, Toh-e A, Tanaka K, Yokosawa H (1998). Growth-dependent change of the 26S proteasome in budding yeast. Biochem Biophys Res Commun 251, 818–823.
Gasch AP, Werner-Washburne M (2002). The genomics of yeast responses to environmental stress and starvation. Funct Integr Genomics 2, 181–192.
Gerlinger UM, Guckel R, Hoffmann M, Wolf DH, Hilt W (1997). Yeast cycloheximide-resistant crl mutants are proteasome mutants defective in protein degradation. Mol Biol Cell 8, 2487–2499.
Gillette TG, Kumar B, Thompson D, Slaughter CA, DeMartino GN (2008). Differential roles of the COOH termini of AAA subunits of PA700 (19 S regulator) in asymmetric assembly and activation of the 26 S proteasome. J Biol Chem 283, 31813–31822.
Goldstein AL, McCusker JH (1999). Three new dominant drug resistance cassettes for gene disruption in *S. cerevisiae*. Yeast 15, 1541–1553.
Groll M, Ditzel L, Lowe J, Stock D, Bochtler M, Bartunik HD, Huber R (1997). Structure of 20S proteasome from yeast at 2.4 A resolution. Nature 386, 463–471.
Hanna J, Leggett DS, Finley D (2003). Ubiquitin depletion as a key mediator of toxicity by translational inhibitors. Mol Cell Biol 23, 9251–9261.
Hanna J, Hathaway NA, Tone Y, Crosas B, Elsasser S, Kirkpatrick DS, Leggett DS, Gygi SP, King RW, Finley D (2006). Deubiquitinating enzyme Ubp6 functions noncatalytically to delay proteasomal degradation. Cell 127, 99–111.
Hardwick JS, Kuruvilla FG, Tong JK, Shamji AF, Schreiber SL (1999). Rapamycin-modulated transcription defines the subset of nutrient-sensitive signaling pathways directly controlled by the Tor proteins. Proc Natl Acad Sci USA 96, 14866–14870.
Herman PK (2002). Stationary phase in yeast. Curr Opin Microbiol 5, 602–607.
Iwanczyk J, Sadre-Bazzaz K, Ferrell K, Kondrashkina E, Formosa T, Hill CP, Ortega J (2006). Structure of the Blm10–20 S proteasome complex by cryo-electron microscopy. Insights into the mechanism of activation of mature yeast proteasomes. J Mol Biol 363, 648–659.
Jorgensen P, Rupes I, Sharom JR, Schneper L, Broach JR, Tyers M (2004). A dynamic transcriptional network communicates growth potential to ribosome synthesis and critical cell size. Genes Dev 18, 2491–2505.
Khor B *et al*. (2006). Proteasome activator PA200 is required for normal spermatogenesis. Mol Cell Biol 26, 2999–3007.
Kisselev AF, Callard A, Goldberg AL (2006). Importance of the different proteolytic sites of the proteasome and the efficacy of inhibitors varies with the protein substrate. J Biol Chem 281, 8582–8590.
Kornitzer D (2002). Monitoring protein degradation. Methods Enzymol 351, 639–647.
Kraft C, Deplazes A, Sohrmann M, Peter M (2008). Mature ribosomes are selectively degraded upon starvation by an autophagy pathway requiring the Ubp3p/Bre5p ubiquitin protease. Nat Cell Biol 10, 602–610.
Kurepa J, Karangwa C, Duke LS, Smalle JA (2010). Arabidopsis sensitivity to protein synthesis inhibitors depends on 26S proteasome activity. Plant Cell Rep 29, 249–259.
Kushnirov VV (2000). Rapid and reliable protein extraction from yeast. Yeast 16, 857–860.
Lam YW, Lamond AI, Mann M, Andersen JS (2007). Analysis of nucleolar protein dynamics reveals the nuclear degradation of ribosomal proteins. Curr Biol 17, 749–760.
Lecker SH, Goldberg AL, Mitch WE (2006). Protein degradation by the ubiquitin-proteasome pathway in normal and disease states. J Am Soc Nephrol 17, 1807–1819.
Lehmann A, Jechow K, Enenkel C (2008). Blm10 binds to preactivated proteasome core particles with open gate conformation. EMBO Rep 9, 1237–1243.
Lempiainen H, Uotila A, Urban J, Dohnal I, Ammerer G, Loewith R, Shore D (2009). Sfp1 interaction with TORC1 and Mrs6 reveals feedback regulation on TOR signaling. Mol Cell 33, 704–716.
Li J, Rechsteiner M (2001). Molecular dissection of the 11S REG (PA28) proteasome activators. Biochimie 83, 373–383.
Li X, Kusmierczyk AR, Wong P, Emili A, Hochstrasser M (2007). β-Subunit appendages promote 20S proteasome assembly by overcoming an Ump1-dependent checkpoint. EMBO J 26, 2339–2349.
Lipford JR, Deshaies RJ (2003). Diverse roles for ubiquitin-dependent proteolysis in transcriptional activation. Nat Cell Biol 5, 845–850.
Longtine MS, McKenzie A III, Demarini DJ, Shah NG, Wach A, Brachat A, Philippsen P, Pringle JR (1998). Additional modules for versatile and economical PCR-based gene deletion and modification in *S. cerevisiae*. Yeast 14, 953–961.
Marion RM, Regev A, Segal E, Barash Y, Koller D, Friedman N, O'Shea EK (2004). Sfp1 is a stress- and nutrient-sensitive regulator of ribosomal protein gene expression. Proc Natl Acad Sci USA 101, 14315–14322.
Marques AJ, Glanemann C, Ramos PC, Dohmen RJ (2007). The C-terminal extension of the β7 subunit and activator complexes stabilize nascent 20 S proteasomes and promote their maturation. J Biol Chem 282, 34869–34876.
Martin DE, Soulard A, Hall MN (2004). TOR regulates ribosomal protein gene expression via PKA and the Forkhead transcription factor FHL1. Cell 119, 969–979.
McCullock S, Kinard T, McCullough L, Formosa T (2006). blm3-1 is an allele of UBP3, a ubiquitin protease that appears to act during transcription of damaged DNA. J Mol Biol 363, 660–672.
McCusker JH, Haber JE (1988). Cycloheximide-resistant temperature-sensitive lethal mutations of *S. cerevisiae*. Genetics 119, 303–315.
Ortega J, Heymann JB, Kajava AV, Ustrell V, Rechsteiner M, Steven AC (2005). The axial channel of the 20S proteasome opens upon binding of the PA200 activator. J Mol Biol 346, 1221–1227.
Pestka S (1971). Inhibitors of ribosome functions. Annu Rev Microbiol 25, 487–562.
Powers T, Walter P (1999). Regulation of ribosome biogenesis by the rapamycin-sensitive TOR-signaling pathway in *S. cerevisiae*. Mol Biol Cell 10, 987–1000.
Rabl J, Smith DM, Yu Y, Chang SC, Goldberg AL, Cheng Y (2008). Mechanism of gate opening in the 20S proteasome by the proteasomal ATPases. Mol Cell 30, 360–368.
Ravid T, Kreft SG, Hochstrasser M (2006). Membrane and soluble substrates of the Doa10 ubiquitin ligase are degraded by distinct pathways. EMBO J 25, 533–543.
Rechsteiner M, Hill CP (2005). Mobilizing the proteolytic machine: cell biological roles of proteasome activators and inhibitors. Trends Cell Biol 15, 27–33.
Rubin DM, Glickman MH, Larsen CN, Dhruvakumar S, Finley D (1998). Active site mutants in the six regulatory particle ATPases reveal multiple roles for ATP in the proteasome. EMBO J 17, 4909–4919.
Rudra D, Zhao Y, Warner JR (2005). Central role of Ifh1p-Fhl1p interaction in the synthesis of yeast ribosomal proteins. EMBO J 24, 533–542.
Sadre-Bazzaz K, Whitby FG, Robinson H, Formosa T, Hill CP (2010). Structure of a Blm10 complex reveals common mechanisms for proteasome binding and gate opening. Mol Cell 37, 728–735.
Schawalder SB, Kabani M, Howald I, Choudhury U, Werner M, Shore D (2004). Growth-regulated recruitment of the essential yeast ribosomal protein gene activator Ifh1. Nature 432, 1058–1061.
Schmidt M, Haas W, Crosas B, Santamaria PG, Gygi SP, Walz T, Finley D (2005). The HEAT repeat protein Blm10 regulates the yeast proteasome by capping the core particle. Nat Struct Mol Biol 12, 294–303.
Schubert U, Anton LC, Gibbs J, Norbury CC, Yewdell JW, Bennink JR (2000). Rapid degradation of a large fraction of newly synthesized proteins by proteasomes. Nature 404, 770–774.
Singh J, Tyers M (2009). A Rab escort protein integrates the secretion system with TOR signaling and ribosome biogenesis. Genes Dev 23, 1944–1958.
Smith DM, Chang SC, Park S, Finley D, Cheng Y, Goldberg AL (2007). Docking of the proteasomal ATPases' carboxyl termini in the 20S proteasome's α ring opens the gate for substrate entry. Mol Cell 27, 731–744.
Stadtmueller BM, Ferrell K, Whitby FG, Heroux A, Robinson H, Myszka DG, Hill CP (2009). Structural models for interactions between the 20S proteasome and its PAN/19S activators. J Biol Chem 285, 13–17.
Stavreva DA *et al*. (2006). Potential roles for ubiquitin and the proteasome during ribosome biogenesis. Mol Cell Biol 26, 5131–5145.

Sutcliffe JA (2005). Improving on nature: antibiotics that target the ribosome. Curr Opin Microbiol 8, 534–542.
Untergasser A, Nijveen H, Rao X, Bisseling T, Geurts R, Leunissen JA (2007). Primer3Plus, an enhanced web interface to Primer3. Nucleic Acids Res 35, W71–74.
Upadhya R, Lee J, Willis IM (2002). Maf1 is an essential mediator of diverse signals that repress RNA polymerase III transcription. Mol Cell 10, 1489–1494.
Ustrell V, Hoffman L, Pratt G, Rechsteiner M (2002). PA200, a nuclear proteasome activator involved in DNA repair. EMBO J 21, 3516–3525.
Wade JT, Hall DB, Struhl K (2004). The transcription factor Ifh1 is a key regulator of yeast ribosomal protein genes. Nature 432, 1054–1058.
Walter J, Urban J, Volkwein C, Sommer T (2001). Sec61p-independent degradation of the tail-anchored ER membrane protein Ubc6p. EMBO J 20, 3124–3131.
Warner JR (1999). The economics of ribosome biosynthesis in yeast. Trends Biochem Sci 24, 437–440.
Whitby FG, Masters EI, Kramer L, Knowlton JR, Yao Y, Wang CC, Hill CP (2000). Structural basis for the activation of 20S proteasomes by 11S regulators. Nature 408, 115–120.
Wullschleger S, Loewith R, Oppliger W, Hall MN (2005). Molecular organization of target of rapamycin complex 2. J Biol Chem 280, 30697–30704.
Xie Y, Varshavsky A (2001). RPN4 is a ligand, substrate, and transcriptional regulator of the 26S proteasome: a negative feedback circuit. Proc Natl Acad Sci USA 98, 3056–3061.
Zhao Y, McIntosh KB, Rudra D, Schawalder S, Shore D, Warner JR (2006). Fine-structure analysis of ribosomal protein gene transcription. Mol Cell Biol 26, 4853–4862.